*Desalination and Water Treatment*
www.deswater.com
doi: 10.1080/19443994.2013.771288

51 (2013) 7137–7144
November

# Application of Ag-doped $TiO_2$ nanoparticle prepared by photodeposition method for nitrate photocatalytic removal from aqueous solutions

Saeed Parastar[a], Simin Nasseri[a,*], Saeedeh Hemmati Borji[a], Mehdi Fazlzadeh[b], Amir Hossein Mahvi[a], Amir Hossein Javadi[c], Mitra Gholami[a]

[a]*Department of Environmental Health Engineering, School of Public Health and Center for Water Quality Research, Institute for Environmental Research (IER), Tehran University of Medical Sciences, Tehran, Iran*
*Tel. +98 2188954914; Fax: +98 2188950188; email: naserise@tums.ac.ir*
[b]*Department of Environmental Health Engineering, School of Public Health and Center for Health, Safety and Environmental, Ardabil University of Medical Sciences, Ardabil, Iran*
[c]*Department of Nanotechnology, Engineering Research Institute, Tehran, Iran*

Received 22 December 2012; Accepted 22 January 2013

## ABSTRACT

Nitrate pollution in surface and groundwater resources is considered as an environmental challenge because of the potential risks of nitrate in diseases such as methemoglobinemia, lymphatic disturbances, and blood cancer. On the other hand, nanomaterials have been recently applied for the control of water pollutants. The objective of this research was to investigate the efficiency of silver-doped $TiO_2$ nanoparticles prepared by photodeposition method under UV irradiation for nitrate removal. Ag-doped $TiO_2$ nanomaterials (Ag/Ti = 0.1 at %) were characterized by scanning electron microscope-energy dispersive X ray, transmission electron microscope, X-ray diffraction, and BET and used in doses of 0.1, 0.4, 0.8, and 1.2 g/L. Three nitrate concentrations of 20, 50, and 100 mg/l were considered in the pH range of 5–9. The effect of Ag-doped $TiO_2$ nanoparticles both in dark and with UV irradiation was studied. Nitrite and ammonia, as intermediates of photocatalytic degradation of nitrate, were detected by spectrophotometric method. Also, in the study, the effect of change in Ag percent doped on $TiO_2$ under UV irradiation for nitrate removal was investigated. The effect of calcination temperature was surveyed on Ag-doped $TiO_2$/UV process efficiency in nitrate removal from aqueous solutions. The optimum performance of nitrate removal (95.5%) was obtained with initial concentration of 100 mg/l and in acidic pH. Increase of Nanoparticle concentration up to 0.8 g/L, improved the removal efficiency, but 1.2 g/l of nanoparticles reduced the degradation efficiency. Maximum reduction performances without nanoparticles (with UV irradiation and in dark) were 32 and 23.3%, respectively. Optimal calcination temperature and optimal silver content doped on $TiO_2$ was obtained at 400°C and 1%.

*Keywords:* Nitrate removal; Photocatalytic process; Ag-doped $TiO_2$; Photodeposition

---

*Corresponding author.

## 1. Introduction

Applications of fertilizers to increase the rate of agricultural products and to respond the food demand growth in different regions of the world have resulted in groundwater pollution problems. High concentrations of nitrate in influent rivers of dam reservoirs have also intensified eutrophication challenges, leading to the decrease of raw water quality in water treatment. The role of nitrate and its organic metabolites in diseases such as methemoglobinemia, lymphatic disturbances, and blood cancer has affected the maximum contaminant level of nitrate in USEPA guidelines 10 mg/l (measured as nitrogen).

Each of conventional techniques for nitrate removal from aqueous solutions, consisting of ion exchange, reverse osmosis, biological denitrification, and chemical reduction has its specific operational or economic constraints [1,2]. Various advanced technologies have been recently applied for water treatment [3]. Photo-assisted catalytic degradation of aqueous contaminants employing semiconductors as photocatalysts is one of the promising technologies [4–6], in which the photocatalytic activity of the catalysts starts with establishing the electron-hole pairs under appropriate illumination [7].

Among various oxide semiconductor photocatalysts, titanium dioxide ($TiO_2$) in the anatase form has been proved to be the most suitable catalyst because of its reasonable photoactivity and being nontoxic, insoluble and comparatively inexpensive [8]. One of the major limitations of $TiO_2$ application in water treatment may be resulted from the effects of relatively large band gap of $TiO_2$, high recombination rate of photogenerated electrons and holes, and low absorption capability of visible light [6,9]. Nanosized $TiO_2$ has recently attracted increasing attention in the field of sensors, ceramics, solar energy conversion, and environmental and pollution control applications [10–14].

In order to improve heterogeneous photocatalysis activity, some surface modification means may be used [15–17]. On the other hand, addition of dopants to $TiO_2$, while maintaining a good control on the nanoscale configurations of the catalyst, may lead to shifting the absorption edge to large wavelengths [3,16–18].

The titanium dioxide nanoparticles have three phases: anatase, rutile, and brokite; anatase and rutile phases are more important due to photocatalytic properties. Photocatalytic process occurs in particles surface; hence in particles surface, crystalline phase is important. One of the effective processes on crystalline structure and particles size is calcination temperature [19]. Intensity of peaks resulting from X-ray diffraction (XRD) analysis determines the ratios of anatase and rutile phases. The ratios of anatase and rutile phases are computed via Spurr and Myers equation [20].

$$\text{Rutile } \% = 100(1 + (0.8 \times I_{\text{A}}/I_{\text{R}}))^{-1} \quad (1)$$

$$\text{Anatase } \% = 100(1 + (1.265 \times I_{\text{R}}/I_{\text{A}}))^{-1} \quad (2)$$

where $I_{\text{A}}$ = anatase peak intensity, $I_{\text{A}}$ = rutile peak intensity.

Many researchers have shown the enhancement of $TiO_2$ photocatalytic activity by impregnating its surface with noble metals and deposition of metals as heterojunction. Result of the study of Tang et al. on photocatalytic reduction of nitrate using Cu-doped titania showed that after 2 h reaction, with the increase of Cu loadings, nitrate removal increases, while a loading of 0.5% is optimal for highest $N_2$ selectivity and TN (total nitrogen) removal [21]. Result of the study investigated by Zhang et al. showed that efficiency of nitrate conversion of Ag-doped $TiO_2$/UV process (UV lamp-125 W and formic acid as hole scavenger) is 98%. Ag-doped $TiO_2$ nanoparticles were synthesized via conventional chemical reduction method. Also, optimal activity of Ag-doped $TiO_2$ was obtained at silver content about 1 wt.% [22]. In another research work, photocatalytic reduction of nitrate in aqueous solution by Au-doped $TiO_2$/UV process was investigated. In this study, using oxalic acid as hole scavenger, although complete elimination of oxalic acid was possible under conditions employed, complete nitrate removal was not achieved [23].

The purpose of this work was to investigate nitrate removal efficiency with common concentration ranges in water resources by the application of Ag-doped $TiO_2$ nanoparticles synthesised via photodeposition method. The effect of pH, initial nitrate concentration, and Ag-doped $TiO_2$ loading were investigated. Also, intermediates of nitrate degradation by this process were detected. Also, in the study, the effect of change in Ag percent doped on $TiO_2$ under UV irradiation for nitrate removal was investigated. Also, the effect of calcination temperature was surveyed on Ag-doped $TiO_2$/UV process efficiency in nitrate removal from aqueous solutions. In the study of Zhang et al., Ag-doped $TiO_2$ nanoparticles were synthesised via conventional chemical reduction method.

## 2. Experimental

### 2.1. Preparation of Ag-doped $TiO_2$ photocatalysts

Raw $TiO_2$ was provided from Nanotechnology Department, Engineering Research Institute in Tehran.

The Ag-doped $TiO_2$ was prepared by photodeposition method [24]. About 46.03 g (1 mol) of formic acid was dissolved in 25 mL deionised water, to which silver nitrate solution ($AgNO_3/HCOOH = 1/10$ at %) was added in dark conditions. Then 200 mL deionised water with 6 g $TiO_2$ were added to the solution. pH was adjusted at 2 by addition of 3.3 mL nitric acid. The solution was mixed for 1 h and was exposed to ultraviolet irradiation (360 nm and 30 W) for 2 h. In this step, silver penetrates within the structure of $TiO_2$ particles. Then the solvent (formic acid) and nitrate were removed from the solution by using filter paper and deionised water. The catalyst was dried at 100°C for three hours in an oven, followed by calcination step under vacuum at $400 \pm 50$°C for three hours. These contents were used for synthesis of Ag-doped $TiO_2$ with the ratio of 0.1 at % (Ag/Ti) [24]. For synthesis of Ag-$TiO_2$ with the ratios of 1 and 3 at % (Ag/Ti), different contents of formic acid and silver nitrate were applied.

### 2.2. Characterization

The surface morphology of the catalyst with ratios of 0.1, 1, and 3 at % (Ag/Ti) was obtained by scanning electron microscope-energy dispersive X ray (SEM-EDX) (Seron Technology AIS-2100). In order to prevent the change build-up during SEM observations, samples were coated with gold. The XRD patterns of the nanocatalysts was determined by a diffractometer (X′ Pert MPD) and the sample morphology and particle size by using a transmission electron microscope (TEM) (ZEISS-EM10C; Accelerating Voltage = 60 kV). The specific surface of Ag-doped $TiO_2$ nanoparticles was determined by BET method (Autosorb 1 Quantachrome).

### 2.3. Photodegradation of nitrate

All of the chemical analyses were done according to standard methods for the examination of water and wastewater [25]. Photoactivity studies were conducted at atmospheric pressure and room temperature (25°C). Photocatalytic degradation experiments were carried out in a 2-L Pyrex batch reactor of cylindrical shape wrapped in aluminum foil to avoid radiation release. A 125-W UV lamp (Trojan) inside a quartz jacket (5 cm inside diameter and 30 cm height) was submerged at the center of the cylindrical vessel (Fig. 1). To provide solution homogeneity, a simple magnetic stirrer was used. A stock solution of potassium nitrate was used for preparation of nitrate solution.

At each experimental stage, 1.5 L solution containing nitrate at designed concentration (20, 50, and 100 mg/l) was prepared by dilution of the stock solution with double distilled water; the experiment was then carried out as follows:

Degradation of nitrate by Ag-doped $TiO_2$/UV: In the first phase, photocatalytic degradation of above-mentioned concentrations of nitrate at three different pH (5, 7, and 9) and with four different concentrations of Ag-doped $TiO_2$ (0.1, 0.4, 0.8, and 1.2 g/L) under UV irradiation was investigated. Also, for study of effect of calcination temperature and change at silver content, experiments were performed at optimal conditions of previous experiments at three different nitrate concentrations (20, 50, and 100 mg/l).

For all experiments, pH was adjusted by NaOH (0.01, 0.1, and 1 N) and HCl (0.01 and 0.1 N). Before irradiation, the suspension was stirred continuously in dark for 30 min to ensure adsorption/desorption equilibrium. After stirring under dark, formic acid as a hole scavenger (0.04 mol/liter) was added into solution. Formic acid is a sacrificial electron donor and has a simple one-carbon molecular structure. Hence, its oxidation to carbon dioxide is straightforward and involves minimal intermediate products [26]. The irradiation time was 180 min and 20 mL of solution was withdrawn from the reactor after 30 min intervals. Liquid samples were centrifuged at 5,000 rpm for 20 min subsequently and filtered (0.2 μm) to separate Ag-doped $TiO_2$ particles. The nitrate concentration in filtrates was measured using UV–Vis spectrophotometer (Perkin-Elmer Lambda 25) at 220 and 275 nm. A quartz cell with a path length of 5 cm was used for spectrophotometeric measurements. Results of this stage led to the determination of optimum pH and photocatalyst concentration. The intermediates of nitrate photocatalytic degradation (nitrite and ammonia) were studied at 543 nm with the above-mentioned spectrophotometer and DR5000, respectively.

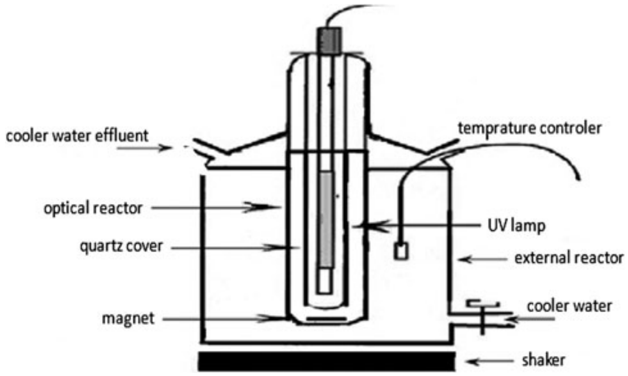

Fig. 1. Schematic diagram of bench-scale photocatalytic reactor.

Degradation of nitrate solely by UV irradiation: for this phase of the study, degradation of nitrate at above-mentioned concentrations and different pH (5, 7, and 9) was investigated under UV irradiation.

## 3. Results and discussion

### 3.1. SEM-EDX, TEM, XRD, and BET analysis

The SEM-EDX images of Ag-doped $TiO_2$ nanoparticles (Fig. 2) suggest its particles size as <19.3 nm. The atomic ratios (at %) of Ag to Ti was estimated as 0.1, 1, and 3. TEM results (Fig. 3) confirm the particles size in agreement with SEM findings (<19.3 nm). Also Table 1 shows crystalline phases formed on Ag-doped $TiO_2$ nanoparticles and their surface area.

### 3.2. Effects of pH, catalyst dose, initial concentration and UV irradiation

Results of pH variation (5, 7, and 9) on nitrate removal efficiency showed the difference of about 10% in the removal efficiency for pH = 5 and pH = 9. The highest removal percentage was obtained at pH = 5 (82%), which was selected for next steps of the experiments. This is attributed to the fact that in acidic pH, TiOH may be present, which reacts with $H^+$ ions as follows:

$$\mathrm{TiOH} + \mathrm{H}^+ \rightarrow \mathrm{TiOH}_2^+ \quad \mathrm{pH}>6.25 \tag{3}$$

$$\mathrm{TiOH} \rightarrow \mathrm{TiO}^- + \mathrm{H}^+ \quad \mathrm{pH}>6.25 \tag{4}$$

The photogenerated electrons during reaction can be captured by the adsorbed $H^+$ to form $H_{oads}$, which is able to reduce nitrate. Fig. 4, presents the effect of catalyst dose on nitrate removal percentage in different irradiation times. Results showed that with increasing catalyst dosage, the nitrate degradation rate increased as a result of the presence of higher numbers of activated absorbed photons and available sites [6,28–30]. Decrease for nitrate degradation catalyst dose of 1.2 g/l compared to 0.8 g/l may be attributed to the opacity and screening effect of excess Ag-doped $TiO_2$ and consequently hindering light penetration leading to the agglomeration of nanoparticles under large catalyst loadings and decreasing the removal efficiency [6,27,28,30,31].

In Fig. 5, the influence of initial nitrate concentration on photocatalytic degradation at three levels (20, 50, and 100 mg/l) is presented. As shown in this figure, nitrate removal decreased with the increase of initial concentration, which may be due to higher rate of light absorption by nitrate (or produced nitrite) for its higher initial concentration [32]. In fact, with progress in reaction especially at high initial concentration, some intermediates are formed and competitively adsorbed on the catalyst surface [33,34].

The effect of catalyst presence on nitrate degradation under UV irradiation is shown in Fig. 6, which presents the positive influence of nanoparticles. This step was carried out for 100 mg/l initial concentration of nitrate, pH = 5 and at 0.1 g/l nanoparticles dose.

Fig. 7 shows the trend of nitrate concentration decrease and simultaneous formation of nitrite and ammonia (as intermediates) up to 0.028 mg/l $NO_2$ and 0.017 mg/l N, followed by decrease in both intermediates concentration. This may be attributed to the fact that a two-steps reaction provides the conversion of nitrate to nitrite, nitrogen, and finally to ammonia. The presence of formic acid as hole scavengers and its

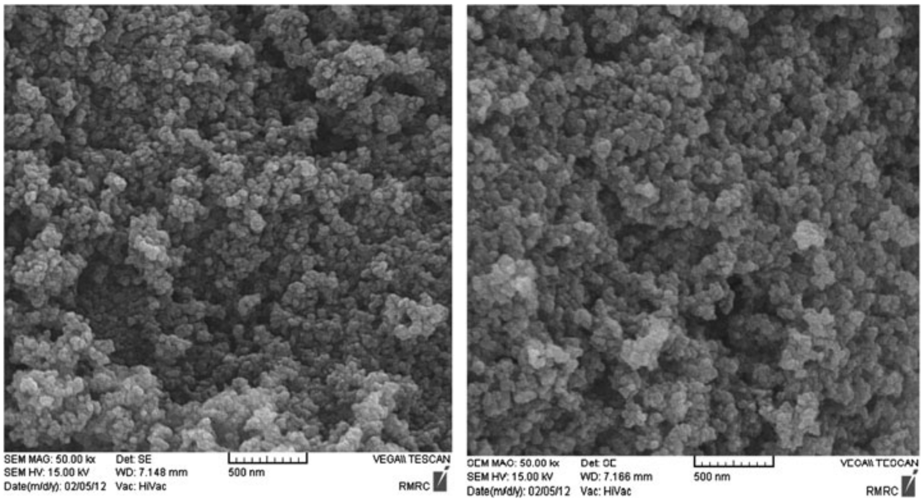

Fig. 2. SEM images of Ag-doped $TiO_2$.

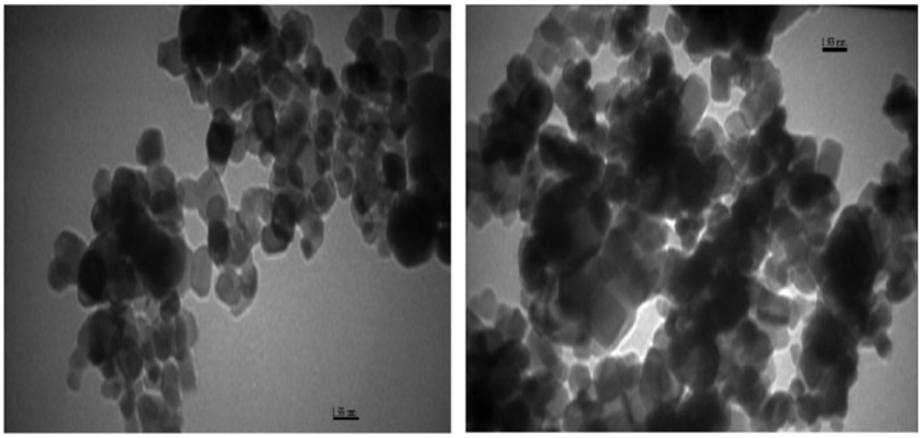

Fig. 3. TEM images of Ag-doped $TiO_2$.

Table 1
The percentage of crystalline phases and nanoparticles surface area at different calcination temperatures

| Calcination temperature (℃) | $I_A$ | $I_R$ | Anatase phase (%) | Rutile phase (%) | BET ($m^2/g$) |
|---|---|---|---|---|---|
| 400℃ (Ag–$TiO_2$ 0.1%) | 1.96 | 2.56 | 37.7 | 62.3 | 64.23 |
| 400℃ (Ag–$TiO_2$ 3%) | 2.65 | 4.2 | 33.27 | 66.45 | 60.09 |
| 200℃ (Ag–$TiO_2$ 1%) | 3.49 | 0.96 | 91.2 | 8.7 | 64.93 |
| 400℃ (Ag–$TiO_2$ 1%) | 1.84 | 5.95 | 74.11 | 25.58 | 54.14 |
| 600℃ (Ag–$TiO_2$ 1%) | 11.67 | 0.89 | 19.64 | 80.16 | 33.66 |

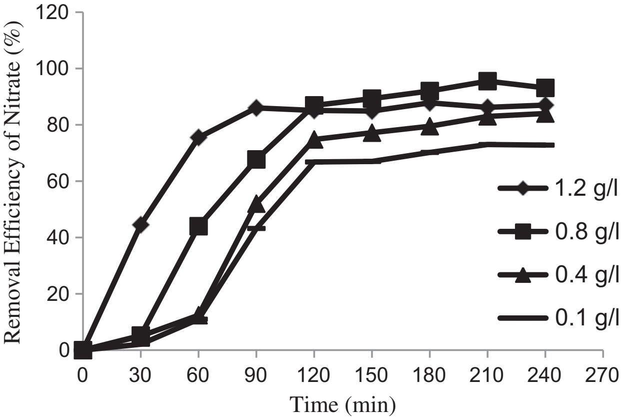

Fig. 4. Effect of catalyst dosage on photocatalytic degradation of nitrate; $C_0 = 100$ mg/l, pH = 5.

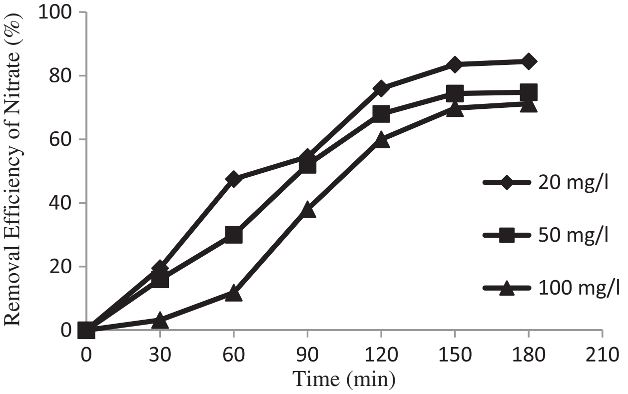

Fig. 5. Effect of initial concentration of nitrate on its photocatalytic degradation; pH = 5 and Ag-doped $TiO_2 = 0.1$ g/l.

concentration within the reactor controls the reduction process; hence, the concentrations of intermediates decrease with time because of formic acid consumption. These results confirm the findings of Rengaraj and Li (2007) that showed the occurrence of the reduction of nitrate via nitrite and ammonia with $Bi^{3+}$–$TiO_2$ nanoparticles in presence of formic acid [35].

### 3.3. The effect of doped silver content and calcination temperature

These experiments was performed in irradiation time 120 min, calcination temperature 400℃, Ag–$TiO_2 = 0.8$ g/l, and pH = 5 for different percents of silver doped on $TiO_2$ (0.1, 1, and 3%) at four different nitrate concentrations. As was observed in Figs. 2 and 3

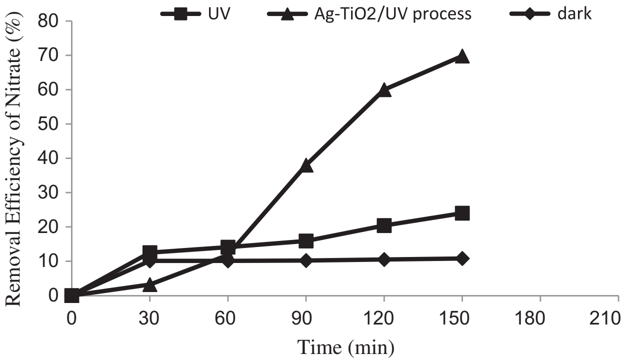

Fig. 6. Effect of catalyst presence on degradation of nitrate under UV irradiation; pH = 5, $C_0 = 100$ mg/l and Ag-doped $TiO_2 = 0.1$ g/l.

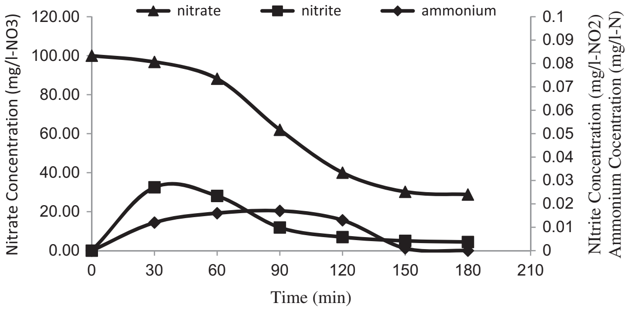

Fig. 7. Intermediates of photocatalytic degradation of nitrate.

(SEM and TEM images), size of Ag–$TiO_2$ (1%) and Ag–$TiO_2$ (3%) is less than 50 nm. As was observed in Fig. 9, nitrate removal efficiency increase in different percents of silver doped on $TiO_2$ 0.1, 3, and 1, respectively.

It may be explained that up to optimum metal loading, the Ag particles deposited on the $TiO_2$ surface can act as electron–hole separation centers. The electron transfer from the $TiO_2$ conduction band to metallic silver particles at the interface is thermodynamically possible because the Fermi level of $TiO_2$ is higher than that of silver metals. These results in the formation of Schottky barrier at the metal-semiconductor contact region, which improve the charge separation and thus enhances the photocatalytic activity of $TiO_2$ [36].

But, the detrimental effect of silver on $TiO_2$ photoactivity that caused Ag-$TiO_2$ (3%) efficiency to be better than Ag–$TiO_2$ (1%) efficiency has several reasons [24]:

- Excessive coverage of $TiO_2$ catalyst by occupying the active sites on the $TiO_2$ surface, limits the amount of light reaching to the surface, reducing the number of photogenerated e-h + pairs and lowering consequently the $TiO_2$ photoactivity.
- Negatively charged silver sites begin to attract holes and subsequently recombine them with electrons. In this case, the metal deposits become recombination centers.
- The probability of the hole capture is increased by the large number of silver particles at high silver loadings, which decrease the probability of holes reacting with adsorbed species at the $TiO_2$ surface.

In a study performed by Sobana and et al. in India in 2008, results show dye removal efficiency increase when silver content is varied as 0.5, 1, 2, and 1.5, respectively [36].

The experiments performed about calcination temperature were accomplished in irradiation time 120 min, Ag–$TiO_2 = 0.8$ g/l (1%) and pH = 5 conditions at calcination temperatures of 200, 400, and 600℃ for four different nitrate concentrations. As was observed in Fig. 8, maximum and minimum of nitrate removal efficiency was obtained at 400 and 200℃, respectively. Many studies have showed that the photocatalytic activity of $TiO_2$ is the function of crystalline phase and grains size. In ratio of anatase to rutile equal to 4:1, photocatalyst has better photocatalytic activity than pure anatase. One of the effective processes on crystalline structure and grains size is calcination temperature of Ag–$TiO_2$ nanoparticle. Under calcination temperature, phase transfer occurs from anatase to rutile [36]. Results show that the rutile phase percent increases and the nanoparticle area decreases with increasing the calcination temperature. Although the nanoparticle area decreases with increasing calcination temperature, but removal efficiency has been corre-

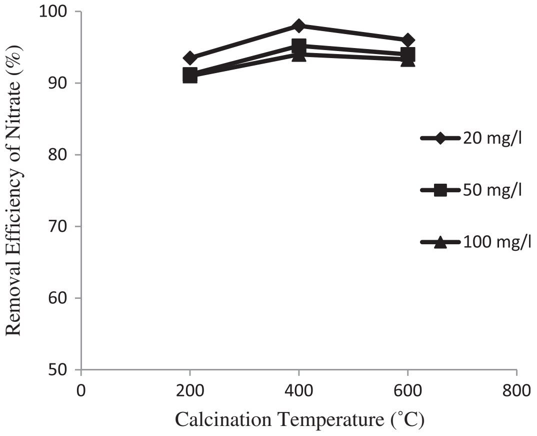

Fig. 8. Effect of calcination temperature on Ag–$TiO_2$/UV process at nitrate removal, $C_0 = 100$ mg/l, pH = 5, (1%) Ag-doped $TiO_2 = 0.8$ g/l.

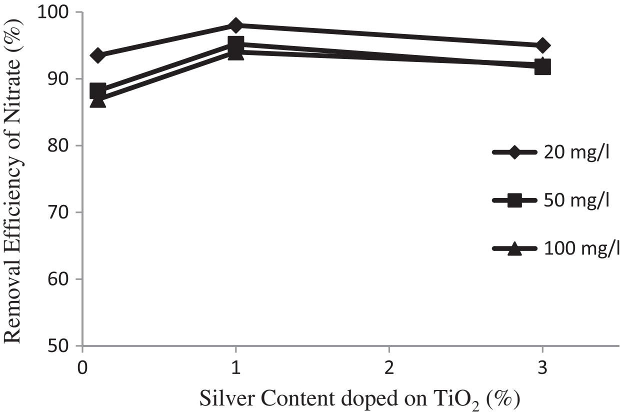

Fig. 9. Effect of silver content on the photoactivity of Ag–$TiO_2$ Nanoparticles at removal of nitrate; pH = 5, $C_0 = 100$ mg/l, and (%) Ag-doped $TiO_2 = 0.8$ g/l.

sponding to ratio of anatase and rutile phases, and maximum removal efficiency has been at calcination temperature 400˚C, the percent of anatase and rutile phases is 74.18 and 28.58%, respectively. Also, this result can be achieved that as particle size increases particles area decreases.

Behnajady and et al. have found that reaction rate constant decreases with increasing calcination temperature from 500 to 900˚C [24]. At the same calcination temperature, the increase of silver content doped on $TiO_2$ do not relate to the ratio of anatase and rutile phases, and also with nanoparticle surface area.

## 4. Conclusion

Photocatalytic degradation of nitrate with Ag-doped $TiO_2$ (produced by photo deposition method) under UV irradiation was carried out. The effects of pH, catalyst dose, and initial nitrate concentration were investigated. At atomic ratio of Ag/Ti = 0.1, photoactivity of Ag-doped $TiO_2$ increased. The highest nitrate degradation efficiency occurred at pH = 5 and 0.8 g/l Ag-doped $TiO_2$ for all different nitrate initial concentrations. The degradation of nitrate decreased with an increase in its initial concentration. The trend of nitrate reduction to the intermediates of nitrite and ammonia was also studied. Also, in this study, results showed that optimal silver content doped on $TiO_2$ is 1% that has better removal efficiency than others. Optimal calcination temperature for Ag–$TiO_2$ was obtained 400˚C.

## Acknowledgments

The authors acknowledge the financial support of the Deputy for Research, Tehran University of the Medical sciences, under Grant No. 13365-27-01-90, and the assistance of the Nanotechnology Department, Engineering Research Institute, in providing Ag-doped $TiO_2$ nanoparticles.

## References

[1] T.D. Reynolds, P.A. Richards, Unit Operations and Processes In Environmental Engineering, PWS, Boston, MA, 1996.
[2] R.D. Letterman, Water Quality and Treatment - A Handbook of Community Water Supplies, fifth ed., McGraw-Hill, New York, NY, 1999.
[3] M. Zhou, J. Yu, B. Cheng, H. Yu, Preparation and photocatalytic activity of Fe-doped mesoporous titanium dioxide nanocrystalline photocatalysts, Mater. Chem. Phys. 93 (2005) 159–163.
[4] S. Sakthivel, M.V. Shankar, M. Palanichamy, B. Arabindoo, D.W. Bahnemann, V. Murugesan, Enhancement of photocatalytic activity by metal deposition: characterisation and photonic efficiency of Pt, Au and Pd deposited on $TiO_2$ catalyst, Water Res. 38 (2004) 3001–3008.
[5] W.C. Hung, S.H. Fu, J.J. Tseng, H. Chu, T.H. Ko, Study on photocatalytic degradation of gaseous dichloromethane using pure and iron ion-doped $TiO_2$ prepared by the Sol-Gel method, Chemosphere 66 (2007) 2142–2151.
[6] S. Nasseri, S. Hemmati, R. Nabizadeh, A.H. Mahvi, A.H. Javadi, Photocatalytic degradation of phenol in aqueous solutions by Fe(III)-doped TiO2/UV process, Proc. of Int. Conf. Nanotech. Fundam. Appl. Ottawa, 2011, 27–29.
[7] M. Behpour, S.M. Ghoreishi, F.S. Razavi, Photocatalytic activity of $TiO_2$/Ag nanoparticle on degradation of water pollutions, Dig. J. Nanomater. Bios. 5 (2010) 467–475.
[8] T.S. Sumita, T.T.Y. Yamaki, S.Y. Yamamoto, Photo induced surface charge separation of highly oriented $TiO_2$ anatase and rutile thin film, Appl. Surf. Sci. 200 (2002) 21–26.
[9] L. Sun, J. Li, C.L. Wang, S.F. Li, H.B. Chen, C.J. Lin, An Electrochemical strategy of doping Fe(III) into $TiO_2$ nanotube array films for enhancement in photocatalytic activity, Sol. Energy Mater. Sol. Cells. 93 (2009) 1875–1880.
[10] L. Miao, P. Jin, K. Kaneko, A. Terai, N. Nabatova-Gabain, S. Tanemura, Preparation and characterization of polycrystalline anatase and rutile $TiO_2$ thin films by RF magnetron sputtering, Appl. Surf. Sci. 212 (2003) 255–263.
[11] N. Perkas, O. Palchik, I. Brukental, I. Nowik, Y. Gofer, Y. Koltypin, A. Gedanken, A mesoporous iron-titanium oxide composite prepared sonochemically, J. Phys. Chem. B. 107 (2003) 8772–8778.
[12] T. Sreethawong, Y. Suzuki, S. Yoshikawa, Photocatalytic evolution of hydrogen over nanocrystalline mesoporous titania prepared by surfactantassisted templating sol–gel process, Catal. Commun. 6 (2005) 119–124.
[13] W. Ho, J.C. Yu, J. Yu, Photocatalytic $TiO_2$/glass nanoflake array films, Langmuir 21 (2005) 3486–3492.
[14] Z. Li, W. Shen, W. He, X. Zu, Effect of Fe-doped $TiO_2$ nanoparticle derived from modified hydrothermal process on the photocatalytic degradation performance on methylene blue, J. Hazard. Mater. 155 (2008) 590–594.
[15] W. Choi, A. Termin, M.R. Hoffman, The role of metal ions dopant in quatum-size $TiO_2$: correlation between photoreactivity and charge carrier recombination dynamics, J. Phys. Chem. 98 (1994) 13669–13679.
[16] D.N. Dvoranova, V.L.S.T. Brezova, M.L. Mazur, Investigation of metal-doped titanium dioxide photocatalysts, Appl. Catal. B. 37 (2002) 91–105.
[17] C. Adan, A. Bahamonde, M. Fernandez-Garcıa, A. Martınez-Arias, Structure and activity of nanosized iron-doped anatase $TiO_2$ catalysts for phenol photocatalytic degradation, Appl. Catal. B. 72 (2007) 11–17.

[18] E. Piera, M.I. Tejedor-Tejedor, M.E. Zorn, M.A. Anderson, Relationship concerning the nature and concentration of Fe (III) species on the surface of $TiO_2$ particles and photocatalytic activity of the catalyst, Appl. Catal. B. 46 (2003) 671–685.

[19] M.M. Shaygani, B. Jaleh, G.H. Ashrafe, The effect of thermal operation and particle size on $TiO_2$ nanoparticle phase changes, J. Majlesi Mater. Eng. 4 (4) (2011) 51–57.

[20] S. Manafi, A.A. Roohani, M. Tabrizi, H. Badiei, Synthesiss and characterization of $TiO_2$ nano-crystal prepared by jelly process, J. Nanocomposite Mater. Res. 1 (2) (2009) 95–102.

[21] L.N. Tang, L.F. Liu, X.Y. Dong, F.L. Yang, Photocatalytic reduction of nitrate using metal-doped titania, 1906863929 PubMed - indexed for MEDLINE, (2011) 2536–2541.

[22] F. Zhang, R. Jin, J. Chen, Ch. Shao, W. Gao, L. Li, N. Guan, High photoactivitic activity and selectivity for nitrogen in nitrate reduction on Ag/$TiO_2$ catalyst with fine silver clusters, J. Catal. 232 (2005) 424–431.

[23] J.A. Anderson, Simultaneous photocatalytic degradation of nitrate and oxalic acid over gold promoted titania, 181 (2012) 171–176.

[24] M.A. Behnajadi, N. Modirshahla, M. Shokri, B. Rad, Enhancement photocatalytic activity of $TiO_2$ nanoparticles by silver doping: photodeposition versus liquid impregnation methods, Global. Nest. J. 10 (2008) 1–7.

[25] A.D. Eaton, L.S. Clesceri, E.W. Rice, A.E. Greenberg, M.A.H. Franson, Standard Methods for The Examination of Water & Wastewater, American Public Health Association, Washington, DC, 2005.

[26] S. Rengaraj, X.Z. Li, Enhanced photocatalytic reduction reaction over $Bi^{3+}$–$TiO_2$ nanoparticles in presence of formic acid as a hole scavenger, Chemosphere 66 (2007) 930–938.

[27] Z. Guo, R. Ma, G. Li, Degradation of phenol by nanomaterial $TiO_2$ in wastewater, Chem. Eng. J. 119 (2006) 55–59.

[28] N. Kashif, F. Ouyang, Parameters effect on heterogeneous photocatalysed degradation of phenol in aqueous dispersion of $TiO_2$, J. Environ. Sci. 21 (2009) 527–533.

[29] A.H. Mahvi, M. Ghanbarian, S. Nasseri, A. Khairi, Mineralization and discoloration of textile wastewater by $TiO_2$ Nanoparticles, Desalination 239 (2009) 309–316.

[30] L. Yang, L.E. Yu, M.B. Ray, Degradation of paracetamol in aqueous solutions by $TiO_2$ photocatalysis, Water Res. 42 (2008) 3480–3488.

[31] Y. Paz, Preferential photodegradation-why and how? C.R. Chim. 9 (2006) 774–787.

[32] K.T. Ranjit, B. Viswanathan, Photocatalytic reduction of nitrite and nitrate ions to ammonia on M/$TiO_2$ catalysts, J. Photochem. Photobiol. A. 108 (1997) 73–78.

[33] D. Chen, A.K. Ray, Photocatalytic kinetics of phenol and its derivatives over UV irradiated $TiO_2$, J. Appl. Catal. B: Environ. 23 (1999) 143–157.

[34] A. Sobczyski, Phenol destruction by photocatalysis on $TiO_2$: an attempt to solve the reaction mechanism, J. Mol. Catal. A: Chem. 213 (2004) 225–230.

[35] N. Sobana, K. Selvam, M. Swaminathan, Optimization of photocatalytic degradation conditions of direct red 23 using nano-Ag doped $TiO_2$, J. Sep. Purif. Technol. 62 (2008) 648–653.

[36] J. Sa, C.A. Aguera, S. Gross, J.A. Anderson, Photocatalytic nitrate reduction over metal modified $TiO_2$, J. Appl. Catal. B: Environ., 85 (3–4) 2009 192–200.